

## **Supporting information**

### **A Compact Planar Low-Energy-Gap Molecule with Donor–Acceptor–Donor Nature Based on a Bimetallic Dithiolene Complex**

Mikihiro Hayashi,<sup>\*,†</sup> Kazuya Otsubo,<sup>†</sup> Tatsuhisa Kato,<sup>□</sup> Kuniyoshi Sugimoto,<sup>§</sup> Akihiko Fujiwara<sup>#</sup> and Hiroshi Kitagawa<sup>\*,†,‡</sup>

<sup>†</sup>*Division of Chemistry, Graduate School of Science, Kyoto University, Kitashirakawa Oiwake-cho, Sakyo-ku, Kyoto 606-8502, Japan*

<sup>§</sup>*Japan Synchrotron Radiation Research Institute (JASRI), SPring-8, 1-1-1 Kouto, Sayo-cho, Sayo-gun, Hyogo 679-5198, Japan*

<sup>□</sup>*Institute for the Promotion of Excellence in Higher Education, Kyoto University, Yoshida-Nihonmatsu, Sakyo-ku, Kyoto 606-8501, Japan*

<sup>#</sup>*Department of Nanotechnology for Sustainable Energy, Graduate School of Science and Technology, Kwansei Gakuin University, Gakuen, Sanda, Hyogo 669-1337, Japan*

<sup>‡</sup>*Core Research for Evolutional Science and Technology (CREST), Japan Science and Technology Agency (JST), 7 Goban-cho, Chiyoda-ku, Tokyo 102-0075, Japan*

### **Contents**

#### **1. Experimental details**

##### **1.1. Materials.**

##### **1.2. Synthesis.**

##### **1.3. <sup>1</sup>H NMR spectra.**

##### **1.4. X-ray single crystal structural analysis.**

##### **1.5. DFT calculation.**

##### **1.6. Electrochemical measurement.**

##### **1.7. Electrolytic absorption measurement.**

##### **1.8. Measurement of electron spin resonance.**

##### **1.9. Apparatus.**

#### **2. Variable temperature resonance Raman spectroscopic measurement.**

#### **3. Temperature dependency of molecular geometry.**

#### **4. Thermal stability.**

#### **5. The result of DFT calculation.**

#### **6. Electrolytic absorption measurement.**

#### **7. Electronic absorption measurement in DMSO and KBr pellet.**

#### **8. Reference.**

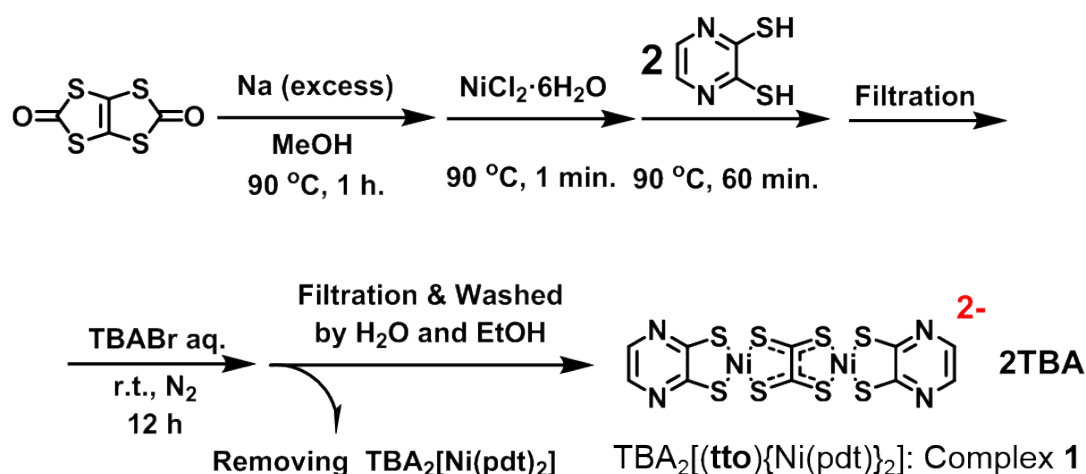
## 1. Experimental details.

### 1.1 Materials.

2,3-pyridine-4,5-dithiolate was prepared according to the previous report<sup>(1)</sup>. In a synthesis, 1,3,4,6-tetrathiapentalene-2,5-dione (TPD) (Tokyo Chemical Industry Co., Ltd.), sodium (Kishida Chemical Co., Ltd.), nickel(II)chloride,6-hydrate (NiCl<sub>2</sub>·6H<sub>2</sub>O) (Wako Pure Chemical Industries, Ltd.), sodium hydroxide (NaOH) (Wako Pure Chemical Industries, Ltd.) and tetrabutylammonium bromide (TBABr) (Wako Pure Chemical Industries, Ltd.) were used without any purification. Water was purified by ion exchange columns. Methanol, dimethylsulphoxide (DMSO) and diethylether at commercially available grade were used. In a NMR measurement, DMSO-d<sub>6</sub> (Wako Pure Chemical Industries, Ltd.) was used. In an electrochemical measurement, tetrabutylammonium perchlorate (TBAClO<sub>4</sub>) (special prepared reagent) (Nacalai Tesque, Inc.), ferrocene (Wako Pure Chemical Industries, Ltd.) and DMSO (infinity Pure grade) (Wako Pure Chemical Industries, Ltd.) were adopted. In a chemically reduced reaction, cobaltocene (CoCp<sub>2</sub>) (Sigma-Aldrich Co. LLC.) and DMSO (for spectrochemical analysis) (Wako Pure Chemical Industries, Ltd.) were used. In an absorption measurement, DMSO (for spectrochemical analysis) (Wako Pure Chemical Industries, Ltd.) and KBr (crystal block) (Wako Pure Chemical Industries, Ltd.) were utilized as diluting agents.

### 1.2 Synthesis.

Tetrabutylammonium( $\mu$ -tetrathiooxarate)bis[(2,3-pyridine-4,5-dithiolato)nickelate(II)];  
TBA<sub>2</sub>[(**tto**){Ni(**pdt**)<sub>2</sub>] (complex **1**)



Under an ambient temperature and an inert atmosphere, 1,3,4,6-tetrathiapentalene-2,5-dione (5.19 g, 25 mmol) was dissolved into a solution of excess amount of sodium in methanol (200 mL). The mixture was stirred at 90°C for 1 hour. During this reaction, the color of solution was changed from light yellow to dark brown. Then, NiCl<sub>2</sub>·6H<sub>2</sub>O (7.58 g, 32 mmol) in methanol (100 mL) and 2,3-pyridine-4,5-dithiolate (7.15 g, 50 mmol) in basic aqueous solution (100 mL) were added to this reaction mixture in this order. After this solution had been stirred for 1 hour at 90°C, an unresolved solid was filtered and tetrabutylammonium bromide (20 g, 62 mmol) in water (100 mL) was added to the filtrate. After this filtered solution had been stirred for 6 hours at ambient temperature, an unresolved solid was generated. By filtration, this solid and filtrate were separated. By evaporating this filtrate, bis(2,3-pyridine-4,5-dithiolato)nickelate(II) (TBA<sub>2</sub>[Ni(pdt)<sub>2</sub>]) was obtained as an orange powder and its single crystal was grown by diffusing gas of diethylether into its acetone solution (7.9 g, 9.6 mmol, 30%). On the other hand, the above mentioned solid was dissolved in acetone, and residue was filtered again. After evaporating acetone from this filtrate, dark brown powder (TBA<sub>2</sub>[(tto){Ni(pdt)<sub>2</sub>}]<sub>2</sub>: complex **1**) was obtained. This residue was recrystallized from DMSO and diethylether to afford rod shaped black crystal (1.2 g, 1.1 mmol, 3.4%). All experiments were performed by use these crystalline samples.

TBA<sub>2</sub>[(tto){Ni(pdt)<sub>2</sub>}]<sub>2</sub> (complex **1**)

<sup>1</sup>H NMR (DMSO-d<sub>6</sub>, 600 MHz): δ = 7.86 (4H, s), 3.15 (16H, m), 1.55 (16H, m), 1.30 (16H, m), 0.92 (24H, t, *J* = 6.4 Hz). Anal. Calcd for C<sub>42</sub>H<sub>76</sub>N<sub>6</sub>Ni<sub>2</sub>S<sub>8</sub>· 2DMSO: C, 73.70; H, 4.92; N, 3.57. Found: C, 73.98; H, 5.09; N, 3.53.

TBA<sub>2</sub>[Ni(pdt)<sub>2</sub>]

<sup>1</sup>H NMR (DMSO-d<sub>6</sub>, 600 MHz): δ = 7.31 (4H, s), 3.18 (16H, m), 1.57 (16H, m), 1.30 (16H, m), 0.91 (24H, t, *J* = 6.4 Hz). Anal. Calcd for C<sub>40</sub>H<sub>76</sub>N<sub>6</sub>NiS<sub>4</sub>: C, 58.02; H, 9.25; N, 10.15. Found: C, 57.79; H, 9.27; N, 10.15.

### 1.3. <sup>1</sup>H NMR spectra.

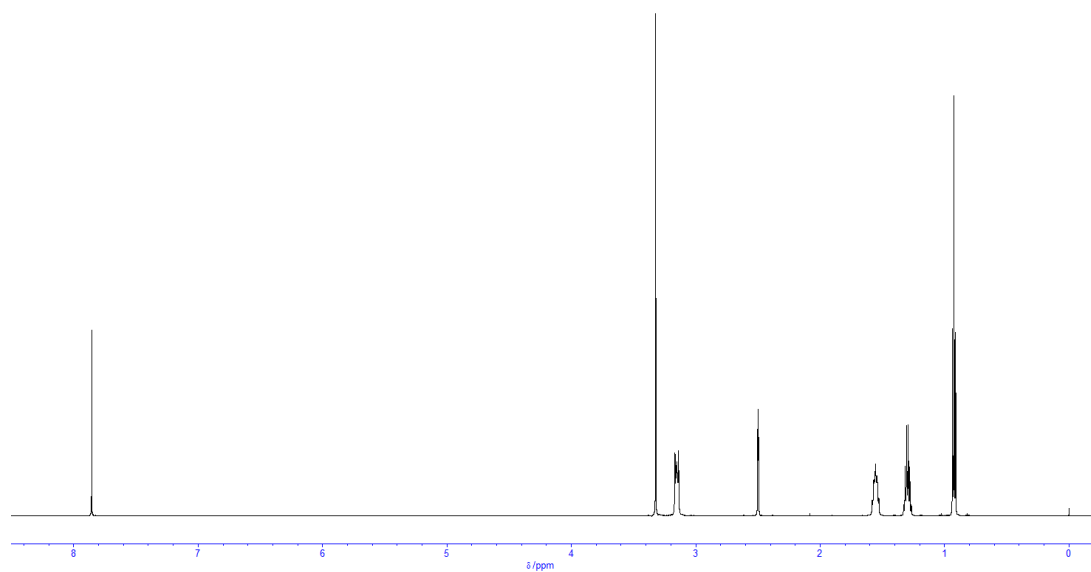


Fig. S1a. <sup>1</sup>H-NMR spectrum of complex **1** in DMSO-d<sub>6</sub>.

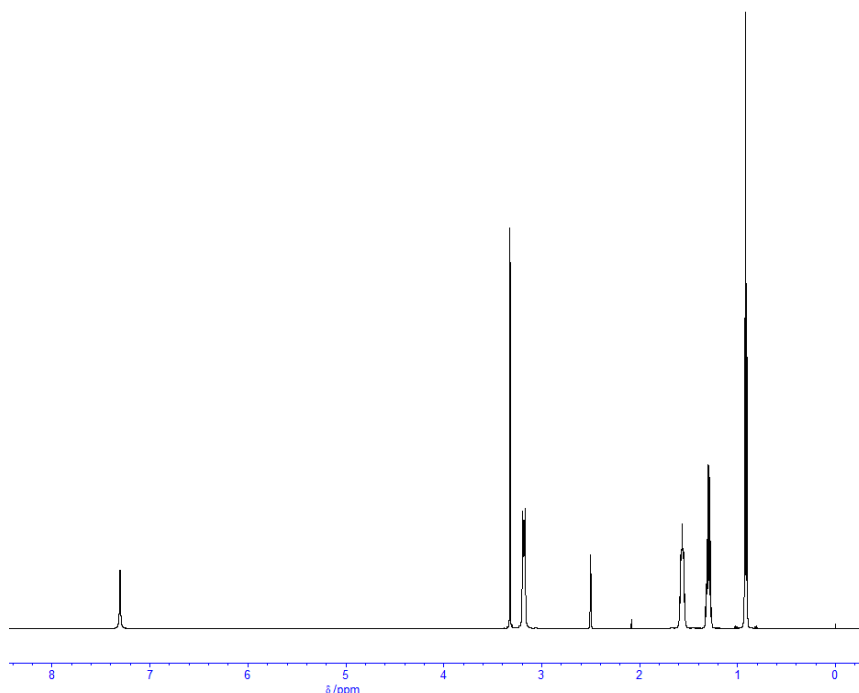


Fig. S1b.  $^1\text{H}$ -NMR spectrum of  $\text{Ni}(\text{pdt})_2\text{TBA}_2$  in  $\text{DMSO-d}_6$ .

#### 1.4. X-ray single crystal structural analysis.

For structural analysis, the diffraction data of single crystal of complex **1** under various temperatures were collected by use of the synchrotron X-ray at the BL02B1 beam-line in SPring-8 with a Rigaku Mercury2CCD detector. In addition, the diffraction data of single crystal of  $\text{TBA}_2[\text{Ni}(\text{pdt})_2]$  at 100 K was collected by use of a Bruker SMART APEX II CCD (charge-coupled device) area detector and a Rigaku AFC-7R Mercury CCD area detector with graphite-monochromated  $\text{Mo } K\alpha$  radiation. Empirical absorption corrections using equivalent reflections and Lorentzian polarization correction were performed using the program Crystal Clear 4.0. The structures were refined against  $F^2$  using SHELXL-97.

#### 1.5. DFT calculation.

The three-parameterized Becke-Lee-Yang-Parr (B3LYP) hybrid exchange-correlation function was employed. As a basis set, 6-31+G (d, p) (C, H, N, S) and Lanl2dz (Ni) were used for  $[(\text{tto})\{\text{Ni}(\text{pdt})_2\}]^{2-}$  and  $[\text{Ni}(\text{pdt})_2]^{2-}$ , on the other hand, 6-31G was used for  $\text{tto}^{2-}$ . The geometries were optimized with symmetry constraints. TD-DFT calculation was executed under the same condition. Solvent effects were not considered in any of the processes.

These calculations were implemented with the Gaussian 09W program.

## **1.6. Electrochemical measurement.**

A series of measurements was carried out in a standard one-component cell, using 3mm $\phi$  glassy carbon (BAS Inc.) as a working electrode, platinum wire (BAS Inc.) as a counter electrode, and Ag/AgClO<sub>4</sub> reference electrode (0.01M AgClO<sub>4</sub> in 0.1M-TBAP/acetonitrile, house-made). As a supporting electrolyte tetrabutylammonium perchlorate was used. As an internal standard, ferrocene was added after each measurement. Electrochemical data were acquired with an ALS 650B voltammetric analyzer (BAS).

## **1.7. Electrolytic absorption measurement.**

In this measurement, a house-made quartz cell with three-electrode system (3mm $\phi$  glassy carbon (BAS Inc.) as a working electrode, platinum mesh (home-made) as a counter electrode, and Ag/AgClO<sub>4</sub> reference electrode (0.01M AgClO<sub>4</sub> in 0.1M-TBAP/acetonitrile, house-made)) was used. As a supporting electrolyte tetrabutylammonium perchlorate was used.

## **1.8. Measurement of Electron spin resonance.**

Electron spin resonance (ESR) spectra of complex **1** and complex **1** with one equivalent of CoCp<sub>2</sub> were measured in frozen DMSO at 8 K. All samples were prepared and measured in an inert condition.

## **1.9. Apparatus.**

NMR study were performed by JEOL spectrometer (600MHz). Absorption spectra were measured with Jasco V-570 UV/Vis spectrometers. Resonant Raman spectra were collected by Jasco NRS-1000 and He-Ne laser ( $\lambda$  = 632 nm) was used for excitation light source. Electrochemical data were acquired with BAS ALS 650B voltammetric analyzer. ESR spectroscopy was recorded by using Bruker EMX, and cryostat ESR 900 of Oxford instrument was utilized for continuous He supply.

## 2. Variable temperature resonance Raman spectroscopic measurement.

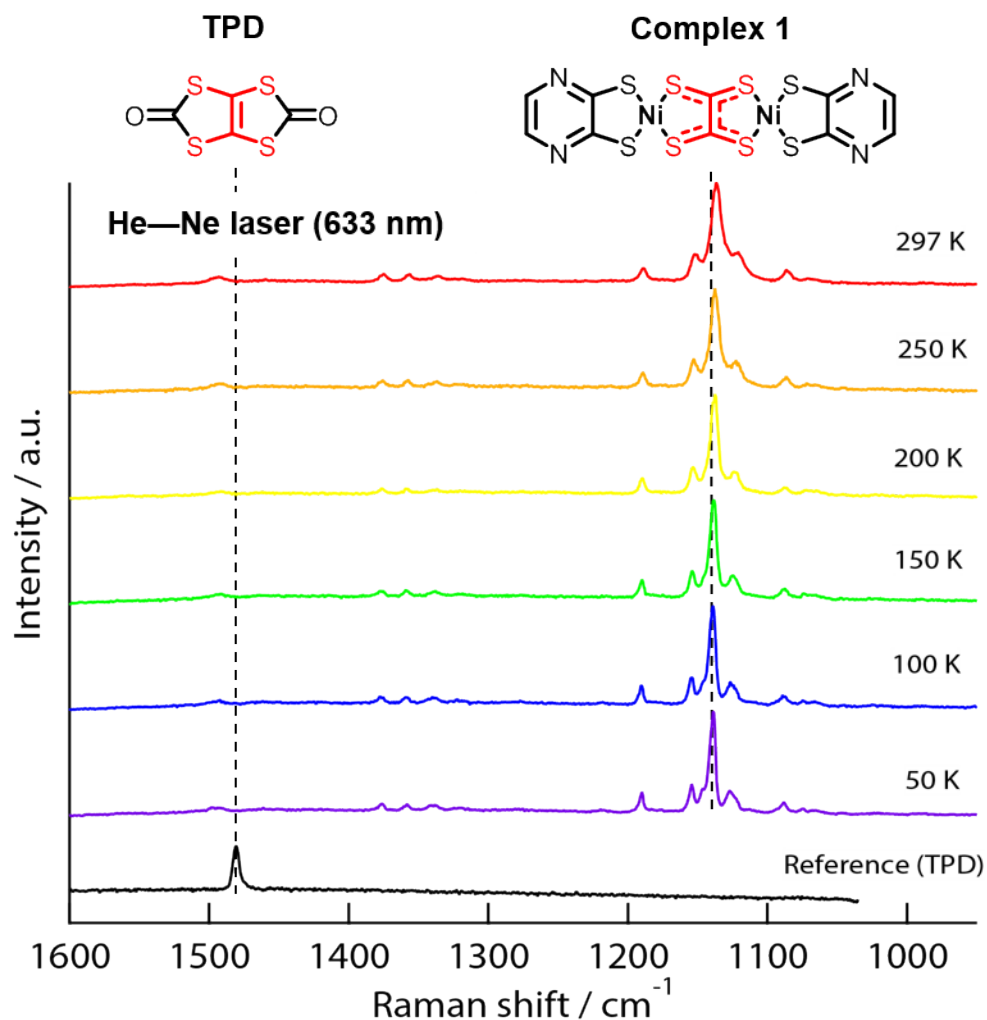


Fig. S2. Resonance Raman spectra of complex **1** from 50 to 297 K. The compared resonance of C-C was observed around 1480  $\text{cm}^{-1}$  by use of 1,3,4,6-tetrathiapentalene-2,5-dione (TPD).

### 3. Temperature dependency of molecular geometry.

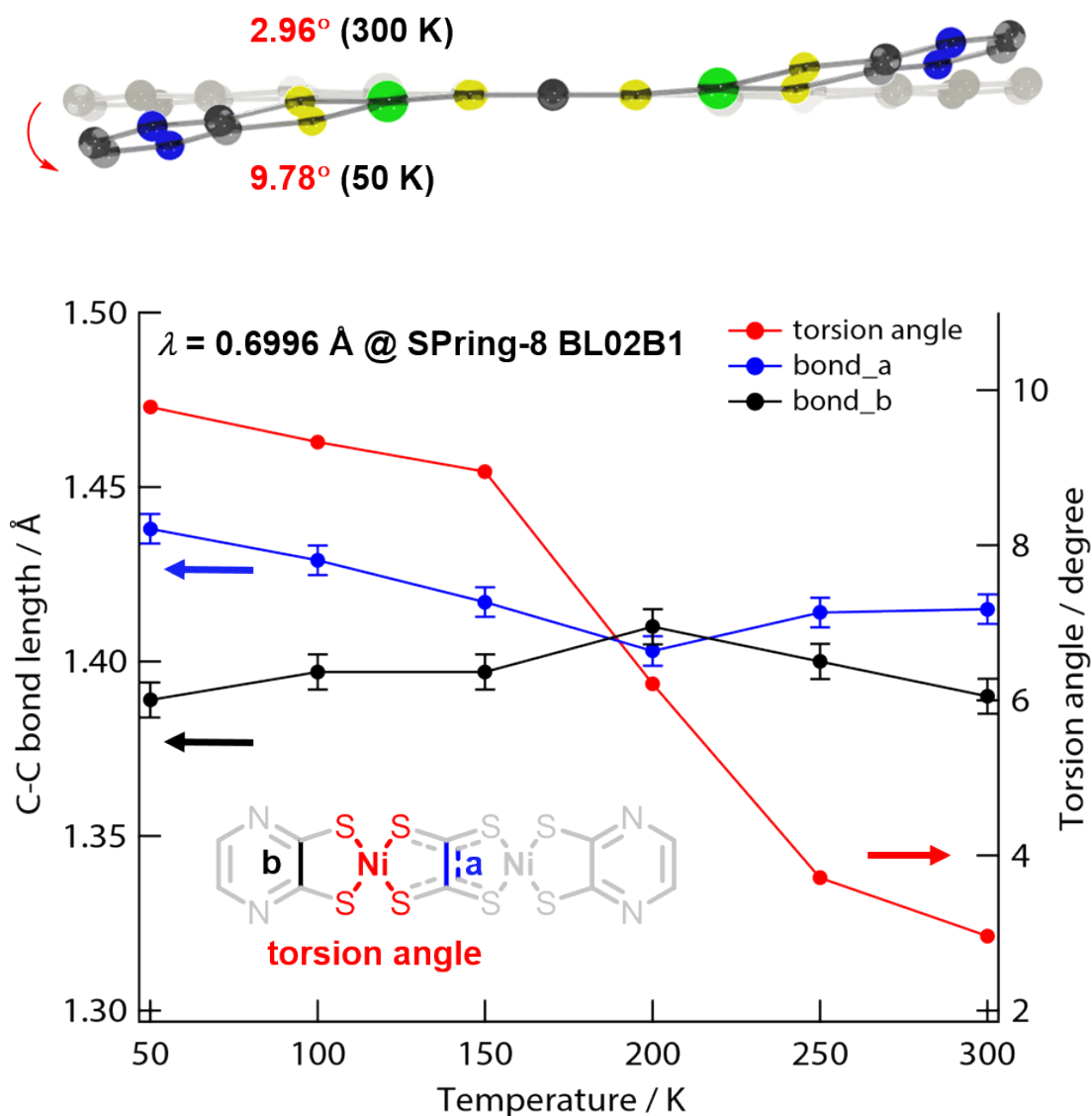


Fig. S3. Temperature dependency of molecular torsion and bond length.

Table S1 Data quality of single crystal X-ray diffraction measurement at SPring-8.

| temperature / K | bond length / Å |          | angle / degree | obtained parameter |       |
|-----------------|-----------------|----------|----------------|--------------------|-------|
|                 | a               | b        | torsion        | R                  | GOF   |
| 300             | 1.415(8)        | 1.39(10) | 2.96           | 0.0755             | 0.840 |
| 250             | 1.416(9)        | 1.40(10) | 3.71           | 0.0901             | 0.920 |
| 200             | 1.397(9)        | 1.41(10) | 6.02           | 0.0902             | 0.976 |
| 150             | 1.417(9)        | 1.397(9) | 8.95           | 0.0911             | 1.028 |
| 100             | 1.429(8)        | 1.397(9) | 9.33           | 0.0878             | 1.057 |



(a) Crystal data of complex **1** @ 50 K:  $C_{46}N_6Ni_2O_2S_{10}$ ; formula weight = 1106.55, monoclinic,  $P2_1/n$ ,  $a = 10.877(3) \text{ \AA}$ ,  $b = 19.073(5) \text{ \AA}$ ,  $c = 13.930(4) \text{ \AA}$ ,  $\beta = 94.607(7)^\circ$ ,  $V = 2880.4(13) \text{ \AA}^3$ ,  $Z = 2$ ,  $D_c = 1.276 \text{ g cm}^{-3}$ , No. of reflections measured = 18,425 (No. of unique reflections = 6536),  $R_1 (I > 2.00\sigma(I)) = 0.0866$ ,  $wR_2 = 0.2407$  (all data), GOF = 1.079.

(b) Crystal data of complex **1** @ 100 K:  $C_{46}N_6Ni_2O_2S_{10}$ ; formula weight = 1106.55, monoclinic,  $P2_1/n$ ,  $a = 10.895(3) \text{ \AA}$ ,  $b = 19.189(5) \text{ \AA}$ ,  $c = 13.957(4) \text{ \AA}$ ,  $\beta = 94.674(7)^\circ$ ,  $V = 2908.3(13) \text{ \AA}^3$ ,  $Z = 2$ ,  $D_c = 1.264 \text{ g cm}^{-3}$ , No. of reflections measured = 18,421 (No. of unique reflections = 6,562),  $R_1 (I > 2.00\sigma(I)) = 0.0878$ ,  $wR_2 = 0.2485$  (all data), GOF = 1.057.

(c) Crystal data of complex **1** @ 150 K:  $C_{46}N_6Ni_2O_2S_{10}$ ; formula weight = 1106.55, monoclinic,  $P2_1/n$ ,  $a = 10.885(4) \text{ \AA}$ ,  $b = 19.278(6) \text{ \AA}$ ,  $c = 13.961(5) \text{ \AA}$ ,  $\beta = 94.810(7)^\circ$ ,  $V = 2919.1(17) \text{ \AA}^3$ ,  $Z = 2$ ,  $D_c = 1.287 \text{ g cm}^{-3}$ , No. of reflections measured = 18,395 (No. of unique reflections = 6,572),  $R_1 (I > 2.00\sigma(I)) = 0.0911$ ,  $wR_2 = 0.2719$  (all data), GOF = 1.028.

(d) Crystal data of complex **1** @ 200 K:  $C_{46}N_6Ni_2O_2S_{10}$ ; formula weight = 1106.55, monoclinic,  $P2_1/n$ ,  $a = 10.7705(17) \text{ \AA}$ ,  $b = 19.924(3) \text{ \AA}$ ,  $c = 13.848(2) \text{ \AA}$ ,  $\beta = 96.499(7)^\circ$ ,  $V = 2952.6(8) \text{ \AA}^3$ ,  $Z = 2$ ,  $D_c = 1.245 \text{ g cm}^{-3}$ , No. of reflections measured = 19,126 (No. of unique reflections = 6,721),  $R_1 (I > 2.00\sigma(I)) = 0.0902$ ,  $wR_2 = 0.2933$  (all data), GOF = 0.976.

(e) Crystal data of complex **1** @ 250 K:  $C_{46}N_6Ni_2O_2S_{10}$ ; formula weight = 1106.55, monoclinic,  $P2_1/n$ ,  $a = 10.7047(15) \text{ \AA}$ ,  $b = 20.555(3) \text{ \AA}$ ,  $c = 13.8324(19) \text{ \AA}$ ,  $\beta = 98.106(7)^\circ$ ,  $V = 3013.2(7) \text{ \AA}^3$ ,  $Z = 2$ ,  $D_c = 1.219 \text{ g cm}^{-3}$ , No. of reflections measured = 19,540 (No. of unique reflections = 6,859),  $R_1 (I > 2.00\sigma(I)) = 0.0901$ ,  $wR_2 = 0.2863$  (all data), GOF = 0.920.

(f) Crystal data of complex **1** @ 300 K:  $C_{46}N_6Ni_2O_2S_{10}$ ; formula weight = 1106.55, monoclinic,  $P2_1/n$ ,  $a = 10.6962(14) \text{ \AA}$ ,  $b = 20.721(3) \text{ \AA}$ ,  $c = 13.8764(19) \text{ \AA}$ ,  $\beta = 98.222(7)^\circ$ ,  $V = 3044.0(7) \text{ \AA}^3$ ,  $Z = 2$ ,  $D_c = 1.207 \text{ g cm}^{-3}$ , No. of reflections measured = 19,774 (No. of unique reflections = 6924),  $R_1 (I > 2.00\sigma(I)) = 0.0755$ ,  $wR_2 = 0.2428$  (all data), GOF = 0.840.

These crystal structures of complex **1** at various temperatures (50, 100, 150, 200, 250 and 300 K) have been deposited at The Cambridge Crystallographic Data Center as publication numbers CCDC 1063807, 1063808, 1063809, 1063810, 1063811 and 1063812.

#### 4. Thermal stability.

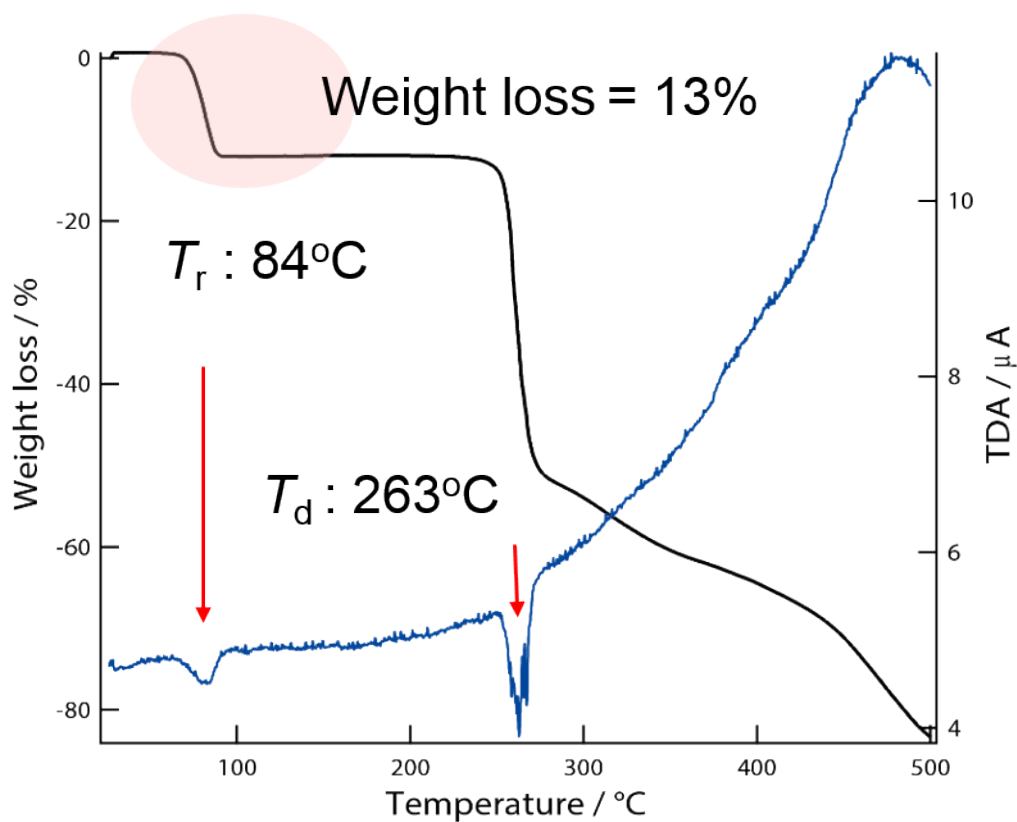


Fig. S4. TG analysis of complex **1**. Desorption temperature ( $T_r$ ) of DMSO molecule and Decomposition temperature ( $T_d$ ) of complex **1** were graphically illustrated. The weight loss of 13% confirmed to the calculated value of DMSO molecule from the result of elemental analysis.

## 5. The result of DFT calculation.

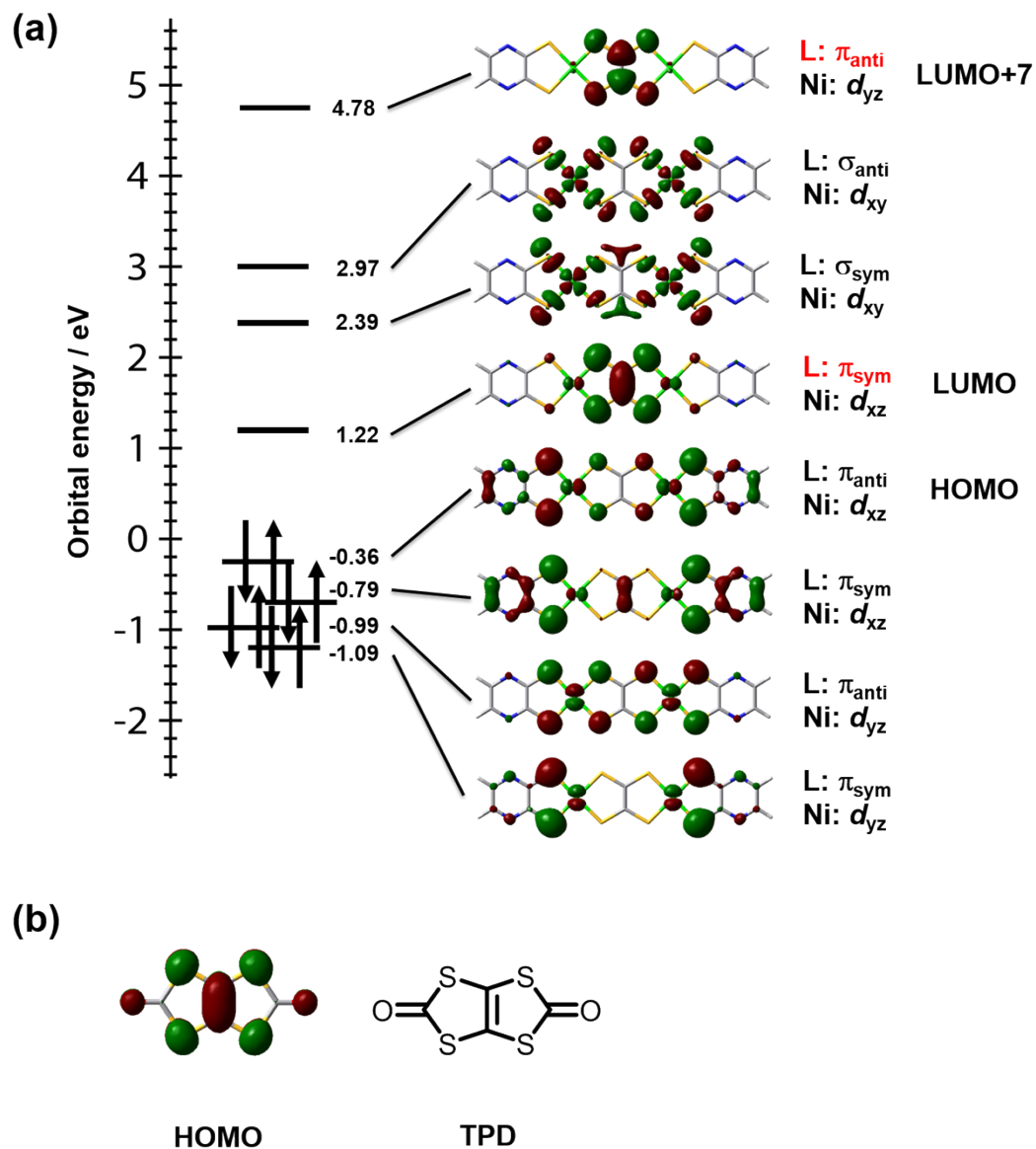


Fig. S5. (a)The result of DFT calculation of complex 1. (b)Calculated HOMO of TPD

The calculation of single point energy of complex **1** with consideration of a solvation effect by DMSO was performed by use of Gaussian 09 with SCRF (PCM,Solvent=DMSO) method. As a result, more reduced energy (0.74 eV) was obtained. This underestimation has often been observed in the result of DFT calculation. This result makes sense because it clearly explains that solvation interaction gives the difference between observed and calculated HOMO–LUMO gap. The result of SCRF calculation was attached as follows.

\*\*\*\*\*

Population analysis using the SCF density.

\*\*\*\*\*

Orbital symmetries:

Occupied (AU) (AG) (AG) (AU) (AG) (AU) (AU) (AG) (AU) (AG)

(AG) (AU) (AU) (AG) (AU) (AG) (AG) (AU) (AG) (AU)

(AG) (AU) (AU) (AG) (AG) (AU) (AU) (AG) (AG) (AU)

(AG) (AU) (AG) (AU) (AU) (AG) (AG) (AU) (AG) (AU)

(AG) (AU) (AG) (AU) (AG) (AU) (AU) (AG) (AG) (AU)

(AG) (AU) (AU) (AG) (AU) (AG) (AG) (AU) (AG) (AU)

(AG) (AU) (AG) (AU) (AG) (AU) (AG) (AU) (AU) (AG)

(AU) (AG) (AU) (AG) (AU) (AG) (AG) (AU) (AG) (AU)

(AG) (AU) (AU) (AG) (AU) (AG) (AU) (AG) (AG) (AU)

(AG) (AU) (AG) (AU) (AU) (AG) (AG) (AU) (AG) (AG)

(AU) (AU) (AG) (AU) (AG) (AU) (AU) (AG) (AG) (AU)

(AU) (AG) (AU) (AG) (AG) (AU) (AU) (AG) (AU) (AG)

(AG) (AU) (AG) (AG) (AU) (AG) (AU) (AU) (AG) (AG)

(AU) (AU) (AG) (AG) (AU) (AU) (AG) (AU) (AG)

Virtual (AG) (AU) (AU) (AG) (AU) (AU) (AG) (AU) (AG) (AU)

(AG) (AU) (AG) (AG) (AU) (AU) (AU) (AG) (AG) (AG)

(AU) (AG) (AU) (AU) (AU) (AG) (AG) (AG) (AU) (AG)

(AU) (AG) (AU) (AG) (AU) (AG) (AU) (AG) (AU) (AG)

(AG) (AU) (AU) (AU) (AG) (AU) (AG) (AU) (AG) (AG)

(AU) (AG) (AG) (AU) (AG) (AU) (AU) (AU) (AU) (AG)

(AG) (AU) (AG) (AU) (AU) (AG) (AG) (AG) (AG) (AU)

(AU) (AU) (AG) (AG) (AU) (AG) (AU) (AU) (AG) (AG)

(AU) (AU) (AU) (AG) (AU) (AG) (AU) (AG) (AU) (AG)

(AG) (AU) (AU) (AG) (AG) (AG) (AU) (AG) (AU) (AU)

(AG) (AG) (AU) (AG) (AU) (AU) (AU) (AG) (AG) (AU)  
 (AG) (AU) (AG) (AU) (AU) (AG) (AU) (AG) (AG) (AU)  
 (AG) (AU) (AG) (AU) (AU) (AG) (AG) (AU) (AG) (AU)  
 (AG) (AU) (AG) (AU) (AG) (AG) (AU) (AU) (AG) (AG)  
 (AU) (AU) (AG)

The electronic state is 1-AG.

|       |                      |           |           |           |           |           |
|-------|----------------------|-----------|-----------|-----------|-----------|-----------|
| Alpha | occ. eigenvalues --  | -89.02677 | -89.02677 | -89.02656 | -89.02655 | -89.02645 |
| Alpha | occ. eigenvalues --  | -89.02644 | -89.02637 | -89.02637 | -16.95161 | -16.84975 |
| Alpha | occ. eigenvalues --  | -14.40883 | -14.40883 | -14.40875 | -14.40875 | -13.09848 |
| Alpha | occ. eigenvalues --  | -13.09674 | -13.06568 | -13.06516 | -13.01565 | -13.01242 |
| Alpha | occ. eigenvalues --  | -10.34201 | -10.34171 | -10.32389 | -10.32389 | -10.32355 |
| Alpha | occ. eigenvalues --  | -10.32355 | -10.27799 | -10.27799 | -10.27750 | -10.27750 |
| Alpha | occ. eigenvalues --  | -9.05920  | -9.05822  | -8.98323  | -8.98251  | -8.97671  |
| Alpha | occ. eigenvalues --  | -8.97624  | -8.94969  | -8.94934  | -8.94582  | -8.94398  |
| Alpha | occ. eigenvalues --  | -8.09141  | -8.09139  | -8.09130  | -8.09129  | -8.09126  |
| Alpha | occ. eigenvalues --  | -8.09125  | -8.09089  | -8.09089  | -6.05629  | -6.05628  |
| Alpha | occ. eigenvalues --  | -6.05617  | -6.05616  | -6.05534  | -6.05534  | -6.05498  |
| Alpha | occ. eigenvalues --  | -6.05497  | -6.04996  | -6.04995  | -6.04985  | -6.04984  |
| Alpha | occ. eigenvalues --  | -6.04934  | -6.04934  | -6.04897  | -6.04897  | -6.04814  |
| Alpha | occ. eigenvalues --  | -6.04814  | -6.04774  | -6.04774  | -6.04682  | -6.04682  |
| Alpha | occ. eigenvalues --  | -6.04670  | -6.04669  | -2.59063  | -2.36105  | -1.04745  |
| Alpha | occ. eigenvalues --  | -1.04739  | -0.97301  | -0.97300  | -0.96051  | -0.91483  |
| Alpha | occ. eigenvalues --  | -0.91008  | -0.89423  | -0.88270  | -0.86042  | -0.85970  |
| Alpha | occ. eigenvalues --  | -0.83941  | -0.80777  | -0.80523  | -0.74075  | -0.70454  |
| Alpha | occ. eigenvalues --  | -0.70382  | -0.70252  | -0.69783  | -0.66156  | -0.63141  |
| Alpha | occ. eigenvalues --  | -0.62128  | -0.60216  | -0.58688  | -0.57419  | -0.57038  |
| Alpha | occ. eigenvalues --  | -0.56630  | -0.55494  | -0.53278  | -0.51991  | -0.51965  |
| Alpha | occ. eigenvalues --  | -0.50957  | -0.48728  | -0.48724  | -0.48490  | -0.47258  |
| Alpha | occ. eigenvalues --  | -0.46103  | -0.46099  | -0.46078  | -0.43018  | -0.42908  |
| Alpha | occ. eigenvalues --  | -0.42638  | -0.42094  | -0.42006  | -0.41231  | -0.40676  |
| Alpha | occ. eigenvalues --  | -0.40584  | -0.40544  | -0.39476  | -0.38599  | -0.37515  |
| Alpha | occ. eigenvalues --  | -0.37043  | -0.35913  | -0.34534  | -0.34530  | -0.34339  |
| Alpha | occ. eigenvalues --  | -0.33407  | -0.32686  | -0.32370  | -0.32148  | -0.31927  |
| Alpha | occ. eigenvalues --  | -0.31403  | -0.28076  | -0.27924  | -0.21495  |           |
| Alpha | virt. eigenvalues -- | -0.18780  | -0.17991  | -0.16068  | -0.15495  | -0.14251  |
| Alpha | virt. eigenvalues -- | -0.12118  | -0.09062  | -0.09049  | -0.08307  | -0.07419  |

|                            |          |          |          |          |          |
|----------------------------|----------|----------|----------|----------|----------|
| Alpha virt. eigenvalues -- | -0.06317 | -0.05808 | -0.05609 | -0.04542 | -0.02146 |
| Alpha virt. eigenvalues -- | -0.00905 | -0.00298 | -0.00137 | 0.01135  | 0.01395  |
| Alpha virt. eigenvalues -- | 0.01745  | 0.01945  | 0.02252  | 0.02526  | 0.02918  |
| Alpha virt. eigenvalues -- | 0.03003  | 0.03840  | 0.03898  | 0.03985  | 0.04459  |
| Alpha virt. eigenvalues -- | 0.05748  | 0.07954  | 0.07955  | 0.11330  | 0.11556  |
| Alpha virt. eigenvalues -- | 0.12901  | 0.14809  | 0.15070  | 0.15437  | 0.15529  |
| Alpha virt. eigenvalues -- | 0.18848  | 0.20052  | 0.21524  | 0.25338  | 0.25866  |
| Alpha virt. eigenvalues -- | 0.27010  | 0.27198  | 0.28544  | 0.28611  | 0.29713  |
| Alpha virt. eigenvalues -- | 0.29991  | 0.30148  | 0.31204  | 0.32098  | 0.32262  |
| Alpha virt. eigenvalues -- | 0.32593  | 0.32757  | 0.32946  | 0.35747  | 0.35929  |
| Alpha virt. eigenvalues -- | 0.36719  | 0.36920  | 0.37338  | 0.37846  | 0.38287  |
| Alpha virt. eigenvalues -- | 0.38655  | 0.41632  | 0.41736  | 0.42267  | 0.42438  |
| Alpha virt. eigenvalues -- | 0.42478  | 0.43101  | 0.43693  | 0.44506  | 0.48353  |
| Alpha virt. eigenvalues -- | 0.48479  | 0.50734  | 0.51436  | 0.51468  | 0.52529  |
| Alpha virt. eigenvalues -- | 0.54352  | 0.54488  | 0.55476  | 0.56271  | 0.57848  |
| Alpha virt. eigenvalues -- | 0.58472  | 0.59197  | 0.59420  | 0.59509  | 0.59620  |
| Alpha virt. eigenvalues -- | 0.60246  | 0.61400  | 0.61909  | 0.62070  | 0.62676  |
| Alpha virt. eigenvalues -- | 0.62876  | 0.63169  | 0.64158  | 0.64660  | 0.64980  |
| Alpha virt. eigenvalues -- | 0.65554  | 0.66061  | 0.69483  | 0.70178  | 0.70293  |
| Alpha virt. eigenvalues -- | 0.74686  | 0.75977  | 0.75983  | 0.77278  | 0.80549  |
| Alpha virt. eigenvalues -- | 0.83290  | 0.83764  | 0.84224  | 0.85224  | 0.85327  |
| Alpha virt. eigenvalues -- | 0.85329  | 0.88923  | 0.88967  | 0.89075  | 0.92493  |
| Alpha virt. eigenvalues -- | 0.92684  | 0.93963  | 0.96912  | 0.97205  | 0.97297  |
| Alpha virt. eigenvalues -- | 0.97533  | 1.03331  | 1.06936  | 1.07034  | 1.11499  |
| Alpha virt. eigenvalues -- | 1.11563  | 1.18934  | 1.19736  | 1.23403  | 1.24086  |
| Alpha virt. eigenvalues -- | 1.29425  | 1.29482  | 1.45610  | 1.45678  | 1.46217  |
| Alpha virt. eigenvalues -- | 1.46460  | 1.82063  | 1.82085  |          |          |

## 6. Electrolytic absorption measurement.

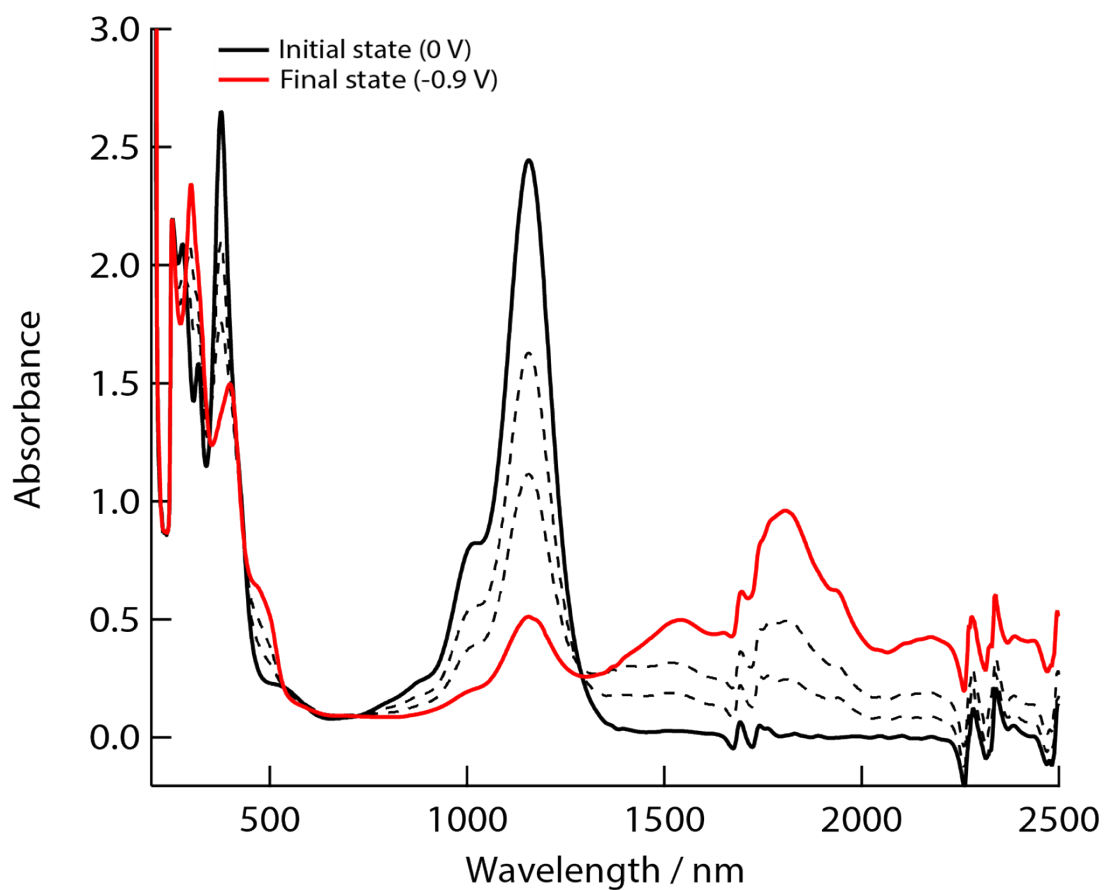


Fig. S6. Electrolytic absorption spectra of complex **1** in 0.1 M  $n\text{Bu}_4\text{NClO}_4$  / DMSO solution under -0.9 V potential (vs.  $\text{Fc}/\text{Fc}^+$ ) at an ambient temperature. Around 1500 nm, broad peak arose corresponding to some transitions involving one electron reduced state of complex **1** as well as chemically reduced measurement in Fig. 3.

## 7. Electronic absorption measurement.

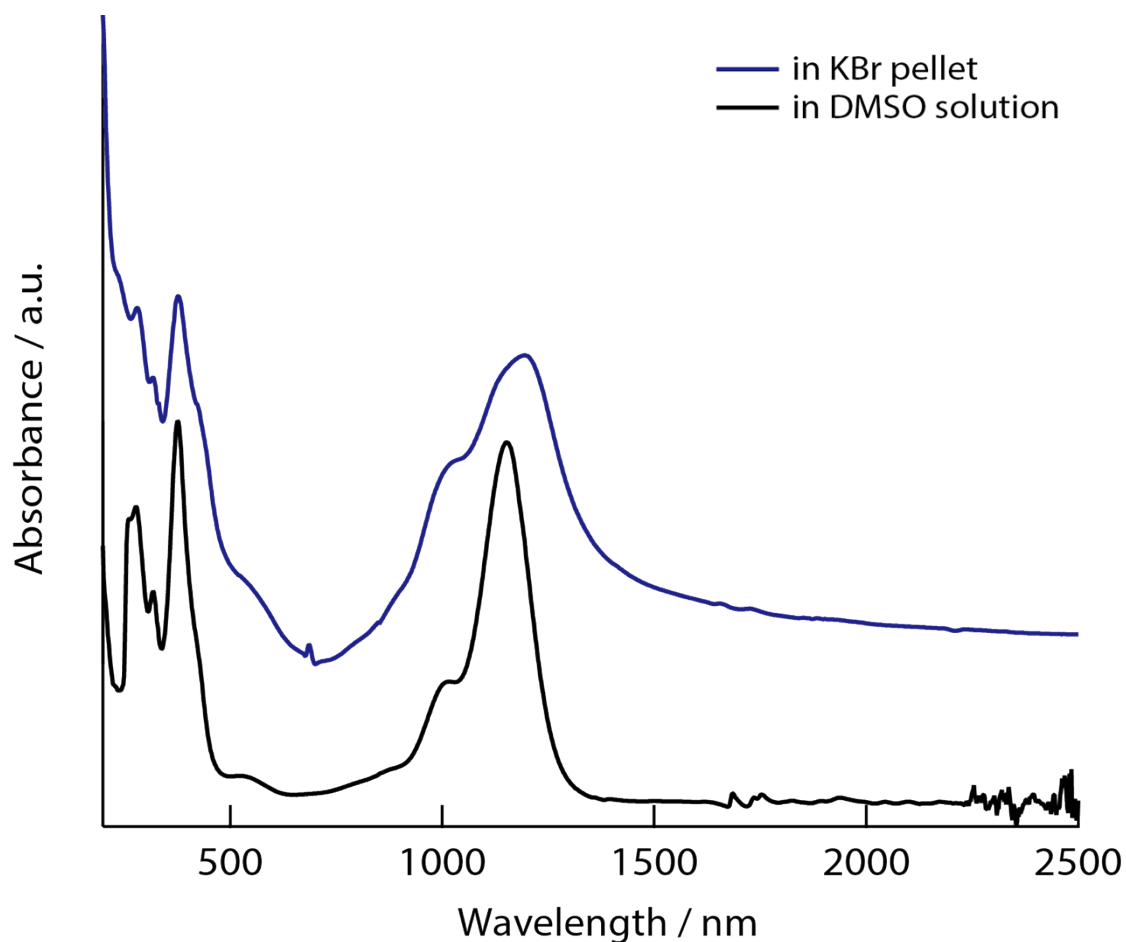


Fig. S7. Electronic absorption spectra of complex **1** in KBr pellet (blue line) and DMSO solution (black line). Most intense peaks around 1150 nm were assigned to the transition from HOMO to LUMO calculated by TD-DFT method.

Table S2. Photochemical data of complex **1**.

| Condition  | Absorption in NIR region |  |
|------------|--------------------------|--|
|            | $\lambda$ / nm           | $\epsilon_{\text{max}}$ / M <sup>-1</sup> cm <sup>-1</sup> |
| KBr pellet | 1182, 1004               | —  |
| DMSO sol.  | 1153, 1004               | 14000, 3300  |

## 8. Reference.

- (1) Y. Kobayashi, B. Jacobs, M. D. Allendorf, J. R. Long, *Chem. Mater.* **2010**, 22, 4120-4122.